JOURNAL OF AIRCRAFT
Vol. 33, No. 2, March–April 1996

Acceleration Techniques for an Aeroelastic Euler Method for a Hovering Rotor

Marilyn J. Smith*
Georgia Institute of Technology, Atlanta, Georgia 30332-0844

Computational fluid dynamics (CFD) methodologies for rotors usually do not permit the rotor to deflect during analysis. However, these deflections do occur in the physical domain and can affect the performance of the rotor. By coupling a Euler code and a structural beam model, these deflections have been incorporated into a CFD simulation. The implementation of the structural beam model is straightforward and can be applied to existing CFD methodologies without extensive effort. However, the cost of the tightly coupled simulation is prohibitive. Techniques to accelerate the convergence of these methods for the quasisteady hover condition are explored. The methods include application of a loosely coupled aeroelastic methodology (vs a tightly coupled methodology), implementation of the full structural deflections using larger update intervals for methodology stability, application of relaxation factors to the full structural deflections, and application of blade deflections predicted by lower-order aerodynamic methods for initial deflections. All of these methods showed some merit, as discussed fully in this article. Aeroelastic analyses with surface deflection updates every 20 iterations provide results that are within 90% of the more expensive tightly coupled analysis results. These methods, while applied to rotors, are also pertinent for fixed-wing applications.

Nomenclature

N = iteration number
R = total blade radius, to blade tip
r = local blade radius
T = local pseudo-time for steady-state solution
β_{pc} = precone angle
β_d = droop angle
ΔT = pseudo-time-step interval

Introduction

THE rotor aeroelastic problem represents one of the most complex aeroelastic problems under present study because of the interaction of the wake, structural dynamics (flexibility), and aerodynamic loads. Most aeroelastic models provide sophistication in one of these areas and rely on simpler representations for the others. Computational fluid dynamics (CFD) simulations, on the other hand, do not permit the input geometry to deflect. Therefore, the actual motion of the full-scale, production rotor cannot be modeled. This can lead to errors in performance estimates using CFD methods.

The introduction of hingeless and bearingless rotors has led to the development of many different aeroelastic analyses. The structural dynamics model developed by Hodges and a number of collaborators is important and is used in a number of research studies. The original beam model was developed by Hodges and Dowell[1] and applied by Hodges and Ormiston.[2] The model was extended for the pitch-link flexible case by Hodges,[3] and used in aeroelastic analyses by Hodges and Ormiston.[4] The model is based on the solution of nonlinear equations of motion for a beam representation of the rotor. These nonlinearities have a significant impact on the aeroelastic predictions. The structural model applied in this research is based on the model described in Ref. 3, with additional corrections developed by de Andrade.[5] No matter how accurate the structural model, the aeroelastic analysis is only as good as the aerodynamic model. The first application of this structural model to aeroelasticity[4] included aerodynamic loads based on the implementation of Greenberg's theory.[6] Greenberg's theory is a modification of Theodorsen's theory[7] and accounts for the time-dependent freestream owing to lead-lag motion and forward flight. The effect of the unsteady wake beneath the rotor can be incorporated by Loewy's[8] unsteady generalization of the Theodorsen function.

In the late 1980s, Kwon[9] improved upon the aeroelastic computations with two-dimensional inflow models (as discussed earlier) by coupling the aeroelastic model of Hodges to a potential-theory-based panel code. This aerodynamic model provided the impact of three-dimensional effects along the blade and at the tip. Wake effects were predicted using the prescribed tip-vortex wake model of Shenoy and Gray.[10]

Kwon's analysis captured part of the large dropoff evident in lead-lag damping observed in the experimental data by Sharpe.[11] The portion of the dropoff that was captured by Kwon was attributed to unsteady three-dimensional aerodynamics. Further studies by de Andrade and Peters[12] have revealed that the remaining discrepancies in the correlations can be corrected by more accurate representations in the lift-curve slope and profile drag (which are input parameters for the code), and refinements in the inflow that account for a recirculating flow that was present in the test section during the original experiments.

During the early 1990s de Andrade[5] developed a finite state inflow model that was compared to the two-dimensional uniform momentum/blade-theory applied by earlier models. Using this model, de Andrade was also able to capture the three-dimensional tip relief effects. However, neither he nor Kwon was able to predict results that correlated favorably with experimental data above 6 deg of collective pitch. This indicated that more complex aerodynamic models may be required to capture the full effect of the flowfield at these higher collective pitch angles.

Other aeroelastic research that has been performed in areas similar to this work include a number of studies by Torok and Chopra[13,14] Their studies also apply two-dimensional aerodynamic theory to a structural model (different from the model of Ref. 3). They have reached an independent conclusion that

Received Nov. 14, 1994; presented as Paper 95-0189 at the AIAA 33rd Aerospace Sciences Meeting and Exhibit, Reno, NV, Jan. 9–12, 1995; revision received Sept. 28, 1995; accepted for publication Oct. 8, 1995.

*Senior Research Engineer, Aerospace Systems Laboratory. Senior Member AIAA.

pressibility in the near-stall regime plays an important role in determining aeroelastic deflections. In 1992, Gea et al.[15] have documented results from a potential flow solver (TFAR2) coupled with a beam model representation of the blade. Both hover and forward-flight simulations were predicted. Little effect in hover was noted using the aeroelastic coupling, although the authors did report that transonic effects were much reduced in forward flight. A planar wake was used to provide the wake information that may account for the small aeroelastic effects in hover.

The focus of this study was to couple the structural beam model of Hodges and Ormiston[4] with an existing CFD solver. This structural model was chosen because of its ease of implementation, as well as its extensive documentation and applications.[1-5,9,16-18] There exist little experimental deflection data for hovering rotors. Thus, the results of the coupled Euler simulations were compared with results of a potential-based panel method[9] that employed the same wake model. This panel method showed excellent correlations with dynamic aeroelastic experiments up to 6–8 deg, but overpredicted the deflections (and damping) at higher angles.[9] Thus, a good basis of comparison exists at lower angles of attack, with trend indicators for higher angles of attack.

Methodology Overview

The aerodynamic and structural dynamics methodologies are not discussed in detail in this article because of space restrictions, but can be found in Ref. 19. Instead, details of the aeroelastic interface between the two methodologies are discussed. The aerodynamic methodology is based on the Reynolds-averaged Navier–Stokes equations that are solved using a spatial fourth-order compact Pade scheme solved using a hybrid alternating direction implicit (ADI) scheme. First- and second-order temporal spacing are available. The aerodynamic code is based on the Euler/Navier–Stokes methodology developed and validated by Wake[20] and later extended to fourth-order in spatial discretization by Smith and Sankar.[21] The grid is a curvilinear grid that is wrapped around each airfoil section using a C-grid and stacked along the rotor radius as an H-grid. Clustering is permitted along the radial, chordwise, and normal directions to resolve the flowfield. The structural dynamics methodology is based on the beam model of Hodges and Ormiston,[3] which has been successfully applied in other applications by de Andrade[5,12] and Kwon.[9]

A flowchart that describes the coupling of the aerodynamic and structural dynamics modules for steady-state hover is shown in Fig. 1. Initially, the aerodynamic and the structural inputs are read in, and the basic input parameters are computed. The values of certain parameters are cross-checked to ensure that the aerodynamic and structural dynamic inputs are compatible. Next, either the rotor blade geometry is read in and the numerical grid computed, or the grid computed via an external code is read in. At this point, the rotor is undeformed and rigid.

Next, the wake data from an external source are read in and interpolated for use in the aerodynamic module. These wake data are based on the flight conditions and blade geometry of the undeformed, rigid rotor. The downwash distribution from the wake is converted to normal and tangential induced velocities that are applied along the radial grid nodes of the rotor blade. For this effort, a momentum inflow wake and a prescribed tip-vortex wake model[10] were applied.

At this point, the computational grid is initialized using the boundary and initial flow conditions. If the solution is restarted from a previous solution, the previous solution flowfield and aeroelastic deformations are read in and serve as the initialized flowfield.

The program next proceeds to iterate using the time option input by the user. For aeroelastic computations, a constant time step throughout the flowfield is necessary so that the deflections remain consistent along the blade surface. The aerodynamics of the flowfield are now computed for given L time steps. For an initial solution L is usually greater than 1 (not a restart). The reason for this is that during the initial steps of the flow solver the loads along the blade will vary greatly as the flowfield rapidly changes. If the aerodynamic loads were introduced into the structural dynamics module at this point, the combination of the rapid flowfield changes and the deforming blade would cause rapid divergence of the blade motion.

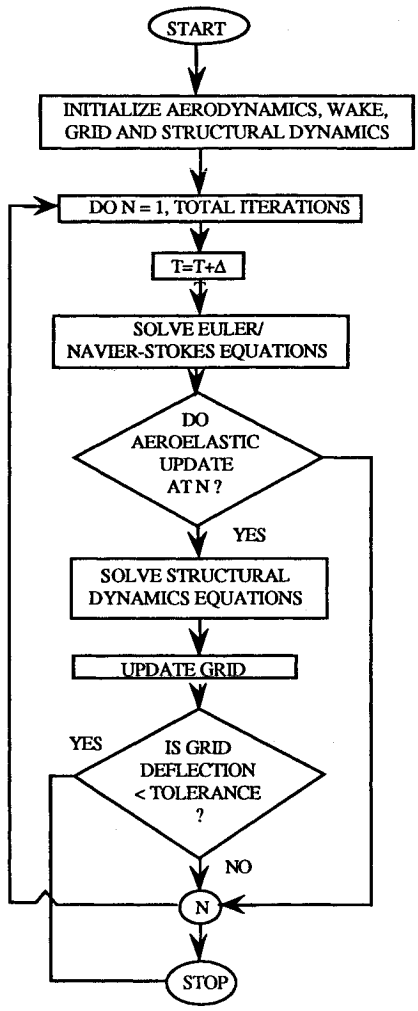

Fig. 1 Schematic that describes the coupling of the Euler aerodynamic module and the structural dynamics module.

Once the aerodynamic flowfield for L iterations has developed, the pressure distribution for all of the grid nodes lying on the blade surface is computed. The structural dynamics module is then called. The structural dynamics module first converts the pressures to aerodynamic loads using the grid cell areas on the blade. These loads are integrated using the mode shapes as weighting functions and applied to the equations that govern the steady-state motion of the elastic hingeless rotor in hover. The blade is represented by a geometrically nonlinear beam model that accounts for coupled flap bending, lead-lag bending, and torsion. Moderately large displacements and rotations because of structural deformations can be simulated. The analysis has been performed for blade configurations having uniform mass and stiffness. The blade was formed by NACA 0012 airfoils.

The aeroelastic governing equations[19] are then differentiated with respect to the equilibrium deflections so that the Jacobian matrix of the equations is obtained. The aerodynamic terms in the Jacobian matrix are neglected since they are not explicitly a function of the equilibrium deflections. Using a coupled iteration with the aerodynamic solver, the residuals of the equa-

tions are computed until they fall below a tolerance level. The deflections of the blade are passed to the grid update routine at each structural dynamics iteration.

The grid update routine takes these deflections and updates the entire computational grid. If the entire grid were not deflected, additional grid motion terms due to differential shearing of the grid would need to be generated. The change in torsion angle is implemented through a change in the downwash angle, rather than an explicit change in the rotation of the blade. This implementation is performed to keep the complexity of the grid updating to a minimum.

The structural dynamics module can be called at the same time steps as the aerodynamic module, or it can be called only every M aerodynamic time steps. The user can vary M. A tightly coupled analysis is obtained when M is set to 1. Higher values of M will update the structure less often, yielding a loosely coupled analysis. For flows that are rapidly varying, calling the structural flexibility every time step can cause unduly large blade deflections.

By implementing this particular methodology, both tightly and loosely coupled aeroelastic analyses can be obtained. A loosely coupled analysis is obtained when a steady-state aerodynamic solution is provided to the structural dynamics solver, and the entire aeroelastic solution is iterated over a minimum of additional flowfield time steps. A tightly coupled analysis is obtained when the aerodynamic flowfield has not yet converged and aeroelastic computations are started. The flexibility of the blade plays an integral part in the evolution of the final steady-state simulation for a tightly coupled solution.

Results

All of the results shown in this section present the deflections that have been nondimensionalized by the radius of the blade.

Loose vs Tight Aeroelastic Coupling

Simulations using the loose and tight coupling procedure discussed in the previous section were run to determine the impact of the feedback computations. Recall that the tightly coupled methodology provides a feedback loop of the aerodynamic loads and structural deflections at every time step. Pressure coefficient plots indicate that the effect of the tightly coupled aeroelastic analyses is to reduce the pressure coefficient suction peaks from those predicted by the rigid blade analysis. This reduction in the pressure peaks is because of an increase in the negative torsion deflection along the blade, shown in Fig. 2a, which creates a slightly nose-down attitude with respect to the loosely coupled analyses. The change in tip-flap deflections is minimal, as seen in Fig. 2b. The largest change is the reduction in tip lead-lag deflections of Fig. 2c. This is because of the reduction of the moment as reflected by the increase in the tip torsional deflection. This nose-down pitching moment causes the blade to move closer towards the local zero angle of attack. As discussed earlier in the Introduction, the panel method does not compare well with Sharpe's dynamic data[11] above 6 deg of collective pitch. Above 8 deg of collective pitch the panel method begins to have problems reaching convergence. This becomes apparent by the nonlinear results at higher collective angles in the lead-lag deflections. At 8 deg of collective pitch and higher, the differences between the panel method and the Euler method simulations become very pronounced. The Euler deflections are in the appropriate direction to correlate better with Sharpe's data.

It is clear from Fig. 2 that a single deflection update (loose coupling) near the end of the CFD analysis does not adequately capture the deflection of the rotor, as signified by the differences in the tightly and loosely coupled data. This method of loose coupling does not capture the feedback effects between the aerodynamic pressures and the deflections. Additional aeroelastic updates are necessary to capture these effects.

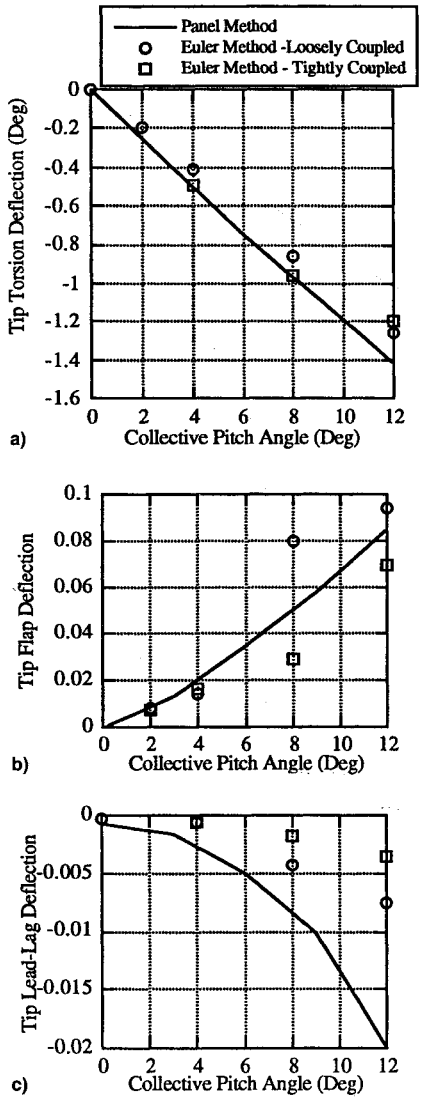

Fig. 2 Euler simulations of a soft inplane rotor at β_{pc} = 0 deg, β_d = 0 deg, 1000 rpm. Equilibrium a) tip torsion, b) tip flap, and c) tip lead-lag deflections.

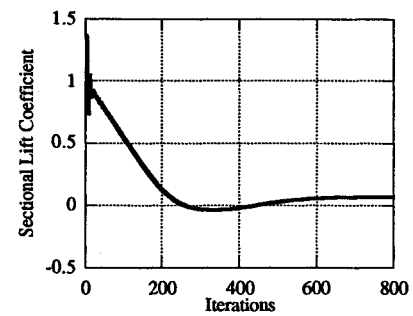

Fig. 3 Rapid change in lift coefficient for a typical radial station as the Euler solutions converge for a rigid blade.

Incremental Aeroelastic Deflection Implementation

Implementing the aeroelastic effects into the Euler aerodynamic module has several disadvantages that are not present in less complex aerodynamic methods. For the Euler rigid blade simulation, the aerodynamic loads change rapidly during initial startup, as seen in Fig. 3. The same effect is felt when the aeroelastic deflections are introduced into the flow solver.

Unlike panel methods, the structural dynamics model and the aerodynamics method cannot be updated at every iteration. The rapid change in the aerodynamic loads causes the aerodynamic solver to diverge as the change in the residual is too large for the hybrid ADI scheme to assimilate. Traditionally, aeroelastic loads have been assimilated into an Euler methodology by multiplying the full deflection by the time step, creating an incremental update scheme. This method requires a large number of iterations to achieve steady state, as shown in Fig. 4. This CPU requirement to solve the steady-state hover problem has resulted in the application of rigid analyses of rotors for higher-order methods, including Euler and Navier–Stokes methods. Two techniques of reducing the impact of the aeroelastic coupling on the aerodynamic solver have been examined to make the inclusion of aeroelastic efforts within the reach of production applications of CFD codes.

The first technique updates the rotor with the entire computed structural deflection, but it increases the number of aerodynamic solver iterations between aeroelastic deflection updates. This provides the code an interval to assimilate the updates and increases the overall robustness of the code. Iteration intervals of 2, 5, 10, 20, and 40 have been examined. The lower iteration intervals of 2, 5, and 10 still cause the code to diverge and the aeroelastic deflections to become nonphysically large. The iteration intervals of 20 and 40 are successful and convergence is reached in 300 to 500 iterations, respectively. Convergence of the aeroelastic code is reached when the average of the nondimensionalized aeroelastic deflection updates for the bending is less than 0.00001. A typical lift coefficient summary for the 20 iteration update is shown in Fig. 5. As the collective pitch angle increases, the number of iterations to reach convergence also increases. This is expected since the aeroelastic updates are larger for the larger collective pitch angles and take longer to reach the same level of convergence.

The second technique assimilates a portion of the aeroelastic deflections that are relaxed from their full values at each update interval. This method passes a portion of the deflections during the initial aeroelastic updates, as defined by a constant multiplication or relaxation factor of 0.0 (no deflection) to 1.0 (100% deflection). It has been postulated that by updating the deflections incrementally, the aerodynamic loads will not change as rapidly during the updates and can be updated with smaller aerodynamic iteration intervals, leading to accelerated convergence. The modification of the sectional lift coefficient is shown in Fig. 6 for a relaxation factor of 0.5 at an update interval of 20 iterations. The updates are much smoother compared with Fig. 5, which has no relaxation factor. Convergence is achieved approximately 50–100 iterations sooner.

Tradeoff studies of relaxation factor and iteration update count have been performed. Using relaxation factors below 0.50 does not yield in faster convergence. Using iteration updates of less than 20 iterations causes the code to become

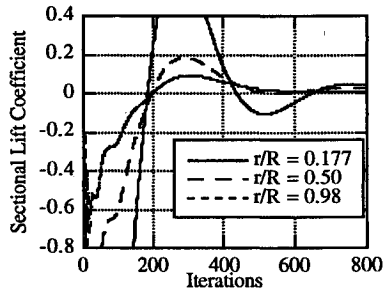

Fig. 4 Using an update interval of 1 iteration and updating deflections by ΔT time increments requires a large number of aeroelastic iterations.

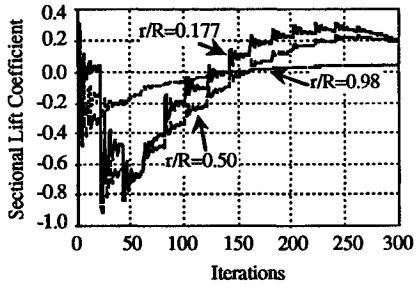

Fig. 5 Sectional lift coefficient summary for coupled Euler aeroelastic computations with deflection updates every 20 aerodynamic iterations.

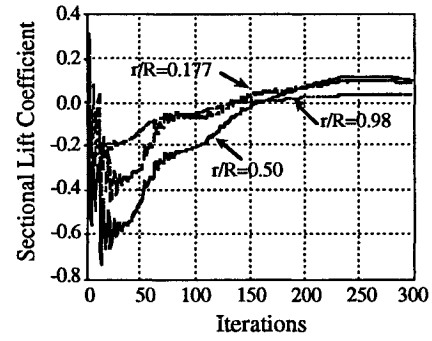

Fig. 6 Sectional lift coefficient summary for coupled Euler aeroelastic computations with deflection updates every 20 aerodynamic iterations using a relaxation factor of 0.5.

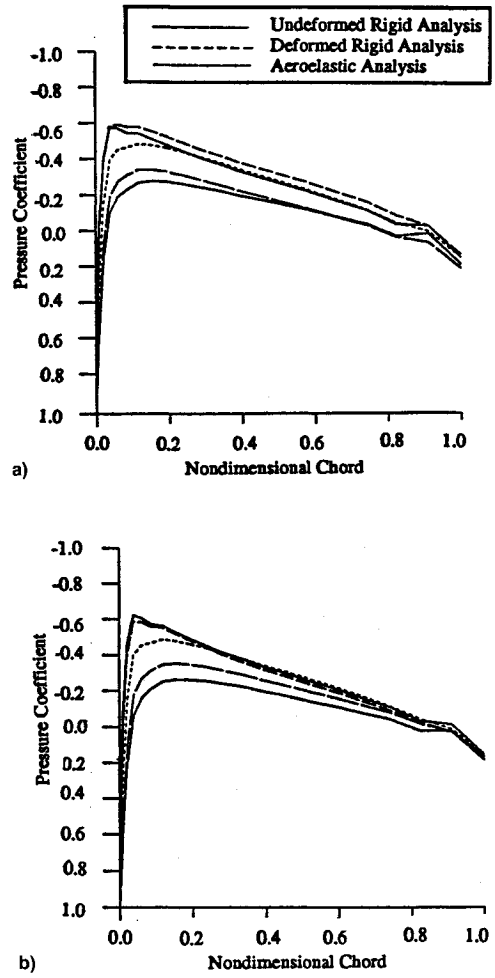

Fig. 7 Comparison of the pressure coefficients predicted by rigid and flexible Euler simulations for 4-deg collective pitch angle: a) 60% radial blade station (r/R = 0.60) and b) 80% radial blade station (r/R = 0.80).

sensitive (lose robustness) at collective angles greater than 8 deg.

Initial Blade Deformations Based on a Dynamic Inflow Model

The higher cost of the Euler aeroelastic method compared with lower-order aeroelastic methods seems very daunting. In an effort to reduce this cost and still include the higher-order aerodynamic effects in the solution result, the dynamic inflow method of de Andrade[5,12] and the Euler methods are loosely coupled to determine the feasibility of this alternative approach. First, the dynamic inflow method at the operational conditions under consideration is run, and the blade deflections are used to generate the initial CFD grid. Then the Euler method for the deflected, but rigid, blade is performed until steady state is achieved. The aeroelastic analysis is then accomplished using either the loose or tight aeroelastic coupling.

The pressure coefficients for the analysis at a collective pitch angle of 4 deg are presented in Fig. 7. Comparisons are made with the Euler simulations of the rigid blade and with the tightly coupled aeroelastic predictions. The effect of the initialization is to begin the reduction of the aerodynamic loads (per the reduction of the suction peak) even during the rigid steady-state phase. The tightly coupled aeroelastic analysis requires only 150–200 iterations to converge for these steady-state solutions of the deformed blade. Update intervals of 20 aerodynamic iterations are still required because of the initial rapid changes made by the aeroelastic updates. Similar results are found for collective pitch angles of 8 and 12 deg. This method of predeforming the blade for the steady-state Euler analyses appears to have merit. The blade deformations, while not totally converged, provide a basis for which the initial steady-state aerodynamic analyses can be performed and reduce the amount of computer time necessary for aeroelastic convergence. The total amount of changes from the initial blade deflections to the final blade deflections is depicted in Figs. 8a–8c for a collective pitch angle of 4 deg.

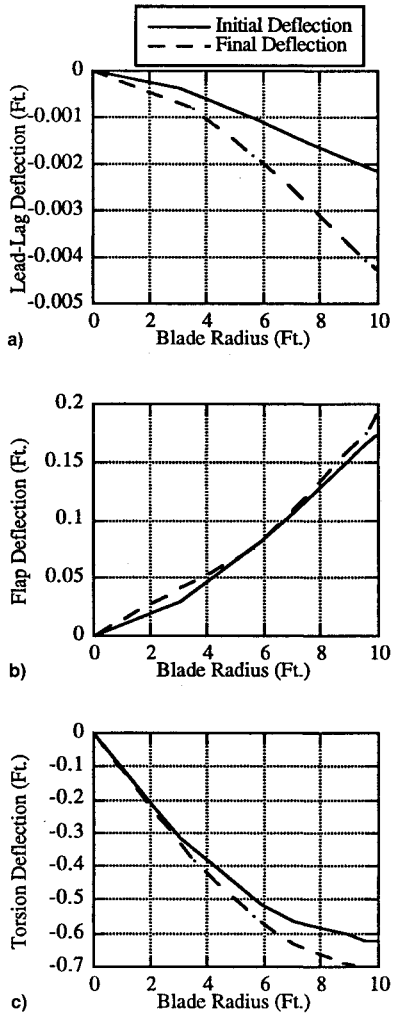

Fig. 8 Euler simulations of a soft in-plane rotor at β_{pc} = 0 deg, β_d = 0 deg, 1000 rpm with and without initial blade deflections computed via a dynamic inflow model. Equilibrium a) lead-lag, b) flap, and c) torsion deflections.

Conclusions

Based on research that has been accomplished and presented in the Results section, the following conclusions have been reached for this simple beam rotor application:

1) A tightly or partially (e.g., updates every 20 iterations) coupled aeroelastic solution must be obtained for collective pitch angles greater than 4 deg. At the lower collective angles (where low lift is implied), a loosely coupled solution captures 90% of the aeroelastic deflections.

2) CPU time reduction can be achieved by including the entire computed aeroelastic deflections at iteration intervals of 20. For higher angles of collective, a relaxation factor between 0.5–1.0 may be required so that the methodology remains robust. This method reduces the number of iterations required to reach equilibrium by 40–50% compared with tightly coupled methods that update partial deflections based on a time-step multiplication factor.

3) CPU time reduction can also be achieved if a lower-order aeroelastic scheme is first used to predict initial offsets. This initial offset can reduce the number of iterations to reach equilibrium by another 25–30%. This initial offset is not adequate to predict aerodynamic aeroelastic deflections.

References

[1]Hodges, D. H., and Dowell, E. H., "Nonlinear Equations of Motion for the Elastic Bending and Torsion of Twisted Nonuniform Rotor Blades," NASA TN D-7818, Dec. 1974.

[2]Hodges, D. H., and Ormiston, R. A., "Stability of Elastic Bending and Torsion of Uniform Cantilever Rotor Blades in Hover with Variable Structural Coupling," NASA TN D-8192, May 1976.

[3]Hodges, D. H., "Nonlinear Equations of Motion for Cantilever Rotor Blades in Hover with Pitch-Link Flexibility, Twist, Precone, Droop, Sweep, Torque Offset and Blade Root Offset," NASA TM X-73, 112, May 1976.

[4]Hodges, D. H., and Ormiston, R. A., "Stability of Hingeless Rotor Blades in Hover with Pitch-Link Flexibility," *AIAA Journal*, Vol. 15, No. 4, 1977, pp. 476–482.

[5]De Andrade, D., "Application of Finite-State Inflow to Flap-Lag-Torsion Damping in Hover," Ph.D. Dissertation, Georgia Inst. of Technology, Atlanta, GA, 1992.

[6]Greenberg, J. M., "Airfoil in Sinusoidal Motion in a Pulsating Stream," NACA TN-1326, 1947.

[7]Theodorsen, T., "The Theory of Propellers," NACA Rept. 775-778, 1944.

[8]Loewy, R. G., "A Two-Dimensional Approximation to the Unsteady Aerodynamics of Rotary Wings," *Journal of Aeronautical Sciences*, Vol. 24, No. 2, 1957, pp. 81–92.

[9]Kwon, O. J., "A Technique for the Prediction of Aerodynamics and Aeroelasticity of Rotor Blades," Ph.D. Dissertation, Georgia Inst. of Technology, Atlanta, GA, 1988.

[10]Shenoy, K. R., and Gray, R. B., "Interactive Lifting Surface Method for Thick Bladed Hovering Helicopter Rotors," *Journal of Aircraft*, Vol. 18, No. 6, 1981, pp. 417–424.

[11]Sharpe, D. L., "An Experimental Investigation of the Flat-Lag-Torsion Aeroelastic Stability of a Small-Scale Hingeless Rotor in Hover," NASA TP-2546, Jan. 1986.

[12]De Andrade, D., and Peters, D. A., "Correlations of Experimental Flap-Lag-Torsion Damping—A Case Study," *Proceedings of the 49th Annual Forum of the American Helicopter Society*, Vol. 2, American Helicopter Society, Washington, DC, 1993, pp. 1011–1028.

[13]Torok, M. S., and Chopra, I., "Rotor Loads Prediction Utilizing a Coupled Aeroelastic Analysis with Refined Aerodynamic Modeling," *Journal of the American Helicopter Society*, Vol. 36, No. 1, 1991, pp. 58–67.

[14]Torok, M. S., and Chopra, I., "Hingeless Rotor Aeroelastic Stability Analysis with Refined Aerodynamic Modeling," *Journal of the American Helicopter Society*, Vol. 36, No. 4, 1991, pp. 48–56.

[15]Gea, L.-M., Chow, C. Y., and Chang, I. C., "Transonic Aeroelasticity Analysis for Rotor Blades," *Journal of Aircraft*, Vol. 29, No. 3, 1992, pp. 477–484.

[16]Peters, D. A., Boyd, D. D., and He, C. J., "Finite-State Induced-Flow Model for Rotors in Hover and Forward Flight," *Journal of the American Helicopter Society*, Vol. 34, No. 4, 1989, pp. 5–17.

[17]Peters, D. A., and Su, A., "Effect of an Unsteady Three Dimensional Wake on Elastic Blade Flapping Eigenvalues in Hover," *Journal of the American Helicopter Society*, Vol. 38, No. 1, 1993, pp. 45–54.

[18]Manjunath, A. R., Nagabhushanam, J., Gaonkar, G. H., Peters, D. A., and Su, A., "Flap-Lag Damping in Hover and Forward Flight with a Three-Dimensional Wake," *Journal of the American Helicopter Society*, Vol. 38, No. 4, 1993, pp. 37–49.

[19]Smith, M. J., and Hodges, D. H., "Development of an Aeroelastic Method for Hovering Rotors with Euler/Navier-Stokes Aerodynamics," *Proceedings of the 51st Annual Forum of the American Helicopter Society*, American Helicopter Society, Washington, DC, 1995.

[20]Wake, B. E., "A Solution Procedure for the Navier-Stokes Equations Applied to Rotors," Ph.D. Dissertation, Georgia Inst. of Technology, Atlanta, GA, 1987.

[21]Smith, M. J., and Sankar, L. N., "Evaluation of a Fourth-Order Compact Operator Scheme for Euler/Navier-Stokes Simulations of a Rotor in Hover," AIAA Paper 91-0766, Jan. 1991.